Short- and medium-range structure of multiferroic Pb(Fe_{1/2}Nb_{1/2})O_{3} studied using neutron total scattering analysis

I.-K. Jeong, J. S. Ahn, B. G. Kim, S. Yoon, Satendra Pal Singh, and Dhananjai Pandey

Short- and medium-range structure of multiferroic $Pb(Fe_{1/2}Nb_{1/2})O_3$ studied using neutron total scattering analysis

I.-K. Jeong[1],[*] J. S. Ahn[2], B. G. Kim[2], S. Yoon[3], and Satendra Pal Singh[4], Dhananjai Pandey[4]

[1] *Department of Physics Education & Research Center for Dielectrics and Advanced Matter Physics,*
Pusan National University, Busan, 609-735, Korea. [2]*Department of Physics,*
Pusan National University, Busan, 609-735, Korea. [3]*Empa,*
Swiss Federal Laboratories for Materials Science and Technology,
Uberlandstrasse, Switzerland. [4]*School of Materials Science and Technology,*
Institute of Technology, Banaras Hindu University, Varanasi,India.
(Dated: December 27, 2010)

We performed neutron total scattering analysis on multiferroic $Pb(Fe_{1/2}Nb_{1/2})O_3$ (PFN) from 300 K to 75 K and present evolution of short- and medium-range atomic structures across antiferromagnetic transition, T_N=143 K. Over the whole temperature range, off-center displacement of Fe/Nb ion was not significant and Fe/Nb-O bond-length distribution exhibits little temperature dependence. In contrast, Pb-O bond length showed a rather distinct distribution at high- and low-temperature. Using a comparison between crystallographic modeling and total scattering pair distribution function analysis we propose that a displacement of Pb ion against Fe/Nb ion is an important low-temperature structural feature. In addition, we present an evidence for a static broadening at T=150 K due to the antiferromagnetic ordering of B-site Fe ion. Overall, we found that Fe/Nb ion plays a role in the multiferroic properties of PFN by influencing off-centering behavior of Pb ion with decreasing temperature.

PACS numbers: 77.84.Dy, 61.43.Gt, 64.70.Kb, 61.12.Ld

I. INTRODUCTION

Lead iron niobate, $Pb(Fe_{1/2}Nb_{1/2})O_3$ (PFN) is one of the most studied multiferroic compounds[1] that uses mixed (magnetically and electrically active) B-site ions to realize the coexistence and coupling of ferroelectric and magnetic orderings[2,3]. PFN exhibits diffuse ferroelectric transition marked by a smeared dielectric response[4] similar to relaxor ferroelectrics, but the dielectric peak temperature T=385 K is frequency independent. As the diffuse nature of the phase transition suggest, polar nanoregions are expected to appear well above the mean transition temperature of 385 K at the so-called Burns temperature[5] which was estimated to be T_d=640 K from temperature dependence of the out-of-plane lattice parameter[6]. As the temperature decreases, PFN undergoes a magnetic transition into antiferromagnetic state at T_N=143 K[7] where a jump in dielectric response was observed, indicating a magnetoelectric coupling[8]. In addition, an anomalous negative thermal expansion[9] was reported below T_N due to a spin-lattice coupling.

The nature of magnetoelectric coupling in PFN was studied by Lente *et al.* using a microwave dielectric spectroscopy and was proposed as an indirect coupling mediated by strain[10]. The importance of lattice strain on the multiferroic properties was also manifested in PFN thin films grown on various $SrTiO_3$ substrates[11]. In this work, enhanced multiferroic properties was observed for films with larger in-plane stress and the enhancement was attributed to distortions of crystal structure. Despite the importance of strain for the multiferroicity in PFN, however, only an average response of lattice was studied across the magnetic ordering transition. So far, no detailed studies on the atomistic picture of the distortion have been reported due to complexities of structural disorder[12,13] of Pb-based ferroelectric compounds.

In this paper, we report short-, and medium-range atomic structure of PFN from 300 K to 75 K using neutron total scattering analysis. Short-range atomic pair distribution showed clear evidence of structural distortion caused by antiferromagnetic ordering of Fe ion below the Néel temperature, T_N. In the medium-range, we observed an abnormal sharpening of certain pair distributions which reflects inter-unit cell atomic ordering and the growth of polar nanoregions with decreasing temperature.

II. EXPERIMENTS AND ANALYSIS

High quality $Pb(Fe_{1/2}Nb_{1/2})O_3$ (PFN) powder sample was prepared using solid state route[14]. Pyrochlore-free single phase was confirmed from x-ray diffraction measurements on powder sample obtained from sintered pellets. Neutron powder diffraction experiments were performed on the NPDF instrument at the Los Alamos Neutron Science Center. For temperature dependent measurements powder sample was loaded in a vanadium can under Helium environment and data were collected at six temperatures from 300 K to 75 K.

Powder diffraction patterns were refined using Rietveld method to obtain long-range structural information such as crystallographic symmetry, lattice constants, atomic positions and thermal parameters. In addition, structural deviation from the long-range order was studied using total scattering (Bragg + diffuse scattering) analysis[15]. As Bragg scattering and diffuse scattering[16] are caused by long-range order and structural disorder, respectively, the total scattering analysis is useful to study atomic structures of disordered crystalline materials[15,17]. In powder diffraction measurements, diffuse scattering is weak and buried underneath strong Bragg peaks. However, the integrated intensity is comparable to Bragg intensities in many of Pb-containing disordered materials[18]. In this work, total scattering structure function, $S(Q)$ which contains both Bragg & diffuse scattering was determined up to wavevector Q=30 Å^{-1} after corrections for experimental effects and normalization by incident neutron flux using program PDFgetN[19]. And then, $S(Q)$ is Fourier transformed into real-space to obtain atomic pair distribution function (PDF) as follows:

$$G(r) = 4\pi r[\rho(r) - \rho_0] = \frac{2}{\pi} \int_0^{Q_{max}} Q[S(Q) - 1]\sin Qr \, dQ. \tag{1}$$

Here, $\rho(r)$, ρ_0, and Q_{max} are the atomic number density, average number density and maximum magnitude of the scattering wavevector, respectively. A peak position of $G(r)$ represents an atomic pair distance and peak width is a measure of mean-square relative displacement due to thermal displacements[20] as well as static disorders.

III. RESULTS AND DISCUSSION

Figure 1 shows neutron powder diffraction pattern of PFN at 75 K (open circles). Solid line represents Rietveld fit using monoclinic Cm space group[9]. Tick mark indicates Bragg peak positions. Also the difference curve is shown. Excellent fitting over wide d-spacing manifests monoclinic crystal structure of PFN. Inset shows temperature

dependence of thermal parameters for Pb^{2+} and Fe^{3+}/Nb^{5+}. Here we note that the thermal parameter of heavier Pb^{2+} ion is a few times larger than that of lighter Fe^{3+}/Nb^{5+} ions at all temperatures. Similar results were reported in previous studies on PFN as well[21]. According to first-principles calculations on Pb-containing perovskite, Pb ions tend to avoid cube faces with high-valence ions and displace toward cube faces with low-valance ions[22]. Thus, Pb ionic displacements are different depending on its nearest-neighbor B-site configurations, resulting in structural disorder. In the Rietveld refinement, the apparent huge thermal parameter of Pb ion is due to a coupling of large static disorder with thermal displacement[23,24].

Next, we move to the total scattering analysis on PFN. Figure 2 (a) shows structure function of PFN at T=75 K with Q_{max}=30 Å^{-1}. Note that at high wavevector diffuse scattering becomes dominant as Bragg peak intensities diminish. The corresponding PDF spectrum is shown in Fig. 2(b). Here, the first PDF peak appears at about 2 Å. Referring to the perovskite-type atomic structure shown in the inset, we can identify that the first PDF peak corresponds to Fe/Nb-O bond length. From the slightly asymmetric shape of the first PDF peak, we can estimate that the B-site off-centering is not significant compared to that observed in relaxor ferroelectric $Pb(Mg_{1/3}Nb_{2/3})O_3$ where the first PDF peak shows a noticeable two-peak structure as a result of Mg/Nb off-centering of about 0.1 Å[17]. The following three Pb-O peaks basically arise due to a Pb off-centering in oxygen twelve cage. The PDF peak at around $r \sim 2.5$ Å indicates that the displacement of Pb ion is quite significant.

For a well-ordered crystalline material, structural information from Rietveld refinement should be consistent with that from the total scattering PDF analysis. In the case of strongly disordered crystalline materials, however, there exists discrepancy in structural information between the two approaches as PDF analysis includes structural disorder. Thus, a direct comparison of experimental PDF and crystallographic model PDF provides useful information on structural disorder. Figure 3(a) shows a comparison between experimental PDF (open circle) and crystallographic model (solid line) PDF at 300 K. The model PDF spectrum was calculated using structural information from Rietveld refinement. Overall, the agreement is acceptable although the shoulder at around $r \sim 2.45$ Å is not well reproduced. Figure 3(b) shows a similar comparison at T=75 K. In the experimental PDF, the broad peak between $3.0 \leq r \leq 3.8$ Å is now split into a doublet. However, the crystallographic model PDF shows only a single peak at the middle ($r \simeq 3.5$ Å) which corresponds to Pb-Fe/Nb pair distance. To remedy the shortcoming of the crystallographic model, we implemented a new feature in the model structure that Pb ion moves away from B-site and displaces to (-0.035, -0.023, -0.025) in the Cm space group. In addition, the thermal parameter of Pb ion is reduced by factor of five. Figure 3(c) shows a new result with much better agreement on Pb-Fe/Nb positions. Here it is worth noting that the fitting quality deteriorates for higher PDF peaks as the off-centering of Pb ion induces additional broadening, which may be related to a static broadening below antiferromagnetic ordering temperature as we discuss in Fig. 4.

Now we discuss temperature evolution of PDF intensity from 300 K to 75 K. Figure 4(a) shows short-range PDF intensity up to pair distance $r \sim 5.3$ Å. Here, we note a few interesting features. Over the whole temperature range, the first PDF peak (Fe/Nb-O bond) shows little temperature dependence. This result indicates that oxygen octahedron is a rigid unit and the central Fe/Nb ion stays more or less at the same site below 300 K. In contrast, the PDF peaks between 3.0 Å< r < 3.8 Å exhibit an interesting evolution with temperature. At T=75 K, PDF peaks are well-resolved as we discussed earlier. Above T=125 K, however, the two-peak feature collapses into one broad hump which looks similar to that of the crystallographic model shown in Fig. 3(a). As the PDF peak distribution in this range is strongly dependent on Pb displacement, we speculate that Pb ion exhibits distinct off-centering behavior at low- and high-temperature, respectively.

In addition, the peak at $r \sim 4.0$ Å exhibits noticeable evolution as a function of temperature. This is an interesting difference between PFN and PMN where almost no temperature dependence was observed for the corresponding peak at $r \sim 4.0$ Å over the similar temperature range[17]. To extract quantitative information, we have fitted the PDF peak using a Gaussian function ($G(x) = A\ Exp[-\frac{(x-x_c)^2}{\sigma^2}]$) and obtained peak width (σ) as a function of temperature. As the contributions from neighboring peaks can influence the fitting result, we fit the peak at $r \sim 4.0$ Å and the neighboring peaks simultaneously. Figure 4(b) shows PDF peak width vs. temperature, $\sigma(T)$. The inset shows the Gaussian fitting of the atomic pair density, $\rho(r)$ in the r-range, 3.5 Å $<$ r $<$ 5.4 Å at 150 K and 175 K, respectively. The PDF peak width shows a strong temperature dependence and gets sharper with decreasing temperature down to T=175 K. With further cooling, however, the peak width does not decrease but becomes a plateau. Since the PDF peak width contains contributions from both thermal and static broadenings, we estimated the thermal contribution to the PDF peak width using the Debye approximation[26]. In Fig. 4(b) the solid line represents an average temperature dependence of a square root of mean-square thermal displacement ($\sqrt{2\langle u^2 \rangle}$)[25] calculated using Eq. (2) with Debye temperatures Θ_D=145 K,

$$\langle u^2 \rangle_{\text{measured}} = \frac{3\hbar}{M\omega_D}\left[\frac{1}{4} + \left(\frac{T}{\Theta_D}\right)^2 \Phi_1\right], \tag{2}$$

where $\Phi_1 = \int_0^{\Theta_D/T} x(e^x - 1)^{-1}\ dx$, $\Theta_D\ (=\hbar\omega_D/k_B)$ is the Debye temperature. Below T=150 K, the deviation of the

PDF peak width from the average temperature dependence becomes clear and we expect that the deviation is due to a lattice distortion related to the antiferromagnetic ordering.

The peak position $r \sim 4.0$ Å corresponds to Fe/Nb-Fe/Nb, Pb-Pb, and O-O pair distances, so we can speculate that one of those pairs is responsible for the static broadening at T=150 K. Among those pairs, we may rule out Fe/Nb-Fe/Nb pair because the ionic displacement of Fe/Nb does not change with temperature. Cooperative tilting of oxygen octahedron can induce the observed broadening below $T = 150$ K but it will accompany long-range structural change[27]. The only pair left is Pb-Pb. As we discussed earlier, Pb off-centering is influenced by B-site Fe/Nb ion. Thus, it is reasonable to speculate that the antiferromagnetic ordering of Fe ions at B-site influences Pb off-centering and increases structural disorder on Pb site leading to the static broadening at T=150 K.

As the pair distance increases larger than the crystallographic lattice parameters, PDF intensity picks up contributions from inter-unit cell atomic ordering. Thus, the temperature evolution of PDF intensity above $r \sim 5.0$ Å provides valuable information on medium-range atomic ordering. In Fig. 5, we notice a peculiar feature. At certain pair distance (e. g. $r \sim 8.99$ Å) PDF peak height shows quite significant temperature dependence compared to peak at other distance (e. g. $r \sim 8.5$ Å). As the area of PDF peak is conserved, the sharp increase of peak height indicates drastic decrease in mean-square relative distance (MSRD) of the corresponding atom pairs. Certainly, MSRD will decrease as temperature is lowered. In this case, however, temperature contribution should be comparable for all pairs beyond the size of unit cell. What we found is that only at certain distances peak height shows strong temperature dependence. Similar temperature evolution of PDF peak height was reported in relaxor ferroelectric $Pb(Mg_{1/3}Nb_{2/3})O_3$ (PMN). In PMN, the intriguing sharpening of PDF peak was interpreted as a result of local structural ordering which leads to the formation of polar nanoregions as well with decreasing temperature. As both PFN and PMN exhibit diffuse dielectric response, we may draw the same conclusion for the temperature dependence in PFN as well i.e. below the maximum temperature of dielectric response ($T_m \sim 387$ K) the volume fraction of polar nanoregions sharply increases due to local structural ordering, and thus PDF peaks get sharper.

IV.   SUMMARY

Using neutron total scattering analysis on multiferroic relaxor $Pb(Fe_{1/2}Nb_{1/2})O_3$, we showed that off-center displacement of Fe/Nb ion is not significant from 300 K to 75 K. Nevertheless, these B-site ions play a role by influencing off-centering behavior of lone pair Pb ion. Due to strong disorder on Pb site, Rietveld refinement alone could not accurately determine the position of Pb ion at low-temperature. In contrast, total scattering analysis clearly demonstrated temperature evolution of atomic pair distances associated with Pb ion. In addition, we presented microscopic picture of the structural response to the antiferromagnetic ordering of B-site Fe ion. On medium-range, PFN exhibits structural feature related to the formation of polar nanoregions with decreasing temperature.

ACKNOWLEDGMENTS

*   To whom correspondence should be addressed. E-mail:Jeong@pusan.ac.kr

[1]   T. Kimura, T. Goto, H. Shintani, K. Ishizaka, T. Arima, and Y. Tokura, Nature **429**, 392 (2003).

[2]   S.-W. Cheong and M. Mostovoy, Nat. Mater. **6**, 13 (2007).

[3]   K. F. Wang, J.-M. Liu, and Z. F. Ren, Advances in Physics **58**, 321 (2009).

[4]   S. P. Singh, A. K. Singh, D. Pandey, H. Sharma, and O. Parkash, J. Mater. Res. **18**, 2677 (2003).

[5]   G. Burns and F. H. Dacol, Solid State Commun. **48**, 853 (1983).

[6]   W. Peng, N. Lemee, M. Karkut, B. Dkhil, V. V. Shvartsman, P. Borisov, W. Kleemann, J. Holc, M. Kosec, and R. Blinc, Appl. Phys. Lett. **94**, 012509 (2009).

[7]   V. A. Vokov, I. E. Mylnikova, and G. A. Smolenskii, Sov. Phys. JETP **15**, 447 (1962).

[8]   Y. Yang, J.-M. Liu, H. B. Huang, W. Q. Zou, P. Bao, and Z. G. Liu, Phys. Rev. B **70**, 132101 (2004).

[9]   S. P. Singh, D. Pandey, S. Yoon, S. Baik, and N. Shin, Appl. Phys. Lett. **90**, 242915 (2007).

[10] M. H. Lente, J. D. S. Guerra, G. K. S. de Souza, B. M. Fraygola, C. F. V. Raigoza, D. Garcia, and J. A. Eiras, Phys. Rev. B **78**, 054109 (2008).

[11] L. Yan, X. Zhao, J. Li, and D. Viehland, Appl. Phys. Lett. **94**, 192903 (2009).

[12] L. E. Cross, Ferroelectrics **76**, 241 (1987).

[13] G. A. Samara, J. Phys: Condens. Matter **15**, R367 (2003).

[14] S. P. Singh, A. K. Singh, and D. Pandy, J. Phys: Condens. Matter **19**, 036217 (2007).

[15] T. Egami and S. J. L. Billinge, *Underneath the Bragg Peaks: Structural Analysis of Complex Materials* (Pergamon Press, Oxfore, UK, 2003).

[16] V. M. Nield and D. A. Keen, *Diffuse Neutron Scattering from Crystalline Materials* (Oxford University Press Inc., New York, 2001).

[17] I.-K. Jeong, T. W. Darling, J. K. Lee, T. Proffen, R. H. Heffner, J. S. Park, K. S. Hong, W. Dmowski, and T. Egami, Phys. Rev. Lett. **94**, 147602 (2005).

[18] D. La-Orauttapong, J. Toulouse, Z.-G. Ye, W. Chen, R. Erwin, and J. L. Robertson, Phys. Rev. B **67**, 134110 (2003).

[19] P. F. Peterson, M. Gutmann, T. Proffen, and S. J. L. Billinge, J. Appl. Cryst. **33**, 1192 (2000).

[20] I.-K. Jeong, Th. Proffen, F. Mohiuddin-Jacobs, and S. J. L. Billinge, J. Phys. Chem. A **103**, 921 (1999).

[21] S. A. Ivanov, R. Tellgren, H. Rundlof, N. W. Thomas, and S. Ananta, J. Phys: Condens. Matter **12**, 2393 (2000).

[22] B. P. Burton, E. Cockayne, S. Tinte, and U. V. Waghmare, Phase Transitions **79**, 91 (2006).

[23] I.-K. Jeong, Phys. Rev. B **79**, 052101 (2009).

[24] H. B. Bürgi, Annu. Rev. Phys. Chem. **51**, 275 (2000).

[25] I.-K. Jeong, R. H. Heffner, M. J. Graf, and S. J. L. Billinge, Phys. Rev. B **67**, 104301 (2003).

[26] P. Debye, Ann. Phys. **39**, 789 (1912).

[27] H. Unoki and T. Sakudo, J. Phys. Soc. Japan **23**, 546 (1967).

FIGURE CAPTIONS

FIG. 1. Neutron powder diffraction pattern of PFN at 75 K (open circle) with the corresponding Rietveld fit using monoclinic Cm space group (solid line). Lattice parameters: a_m=5.6775(2) Å; b_m=5.6620(2) Å; c_m=4.0168(1) Å; $\alpha=\gamma=90°$, $\beta=90.246(2)°$. Atomic positions: Pb^{2+} (0.0,0.0,0.0), Fe^{3+}/Nb^{5+} (0.519(2), 0.0, 0.463(2)), O_I^{2-} (0.525(2), 0.0, -0.035(2)), O_{II}^{2-} (0.294(2), 0.256(1), 0.429(2)). R_{wp} = 4.31 %, R_p = 3.10 %. Tick mark for peak positions and difference curve are also shown. Inset shows thermal parameters of Pb and Fe/Nb ions from 300 K to 75 K. Note that the thermal parameter of heavier Pb ion is much larger than that of lighter Fe/Nb ion. This result indicates the existence of static disorder on Pb site.

FIG. 2. (a) Structure function, $Q[S(Q)$-1] of PFN at 75 K. (b) Experimental PDF spectrum. The first few PDF peaks correspond to Fe/Nb-O, (Pb-O, O-O), and Fe/Nb-Pb bond lengths. Refer to perovskite-type atomic structure shown in the inset of (a).

FIG. 3. (a) Comparison between experimental PDF (open circle) and crystallographic model PDF (solid line) at 300 K. For the model PDF calculation, structural information from Rietveld refinement was used. (b) Experiment vs. crystallographic model PDF at 75 K. Note that the broad peak between $3.0 \leq r \leq 3.8$ Å is now split into a doublet at 75 K in the experimental PDF spectrum. However, crystallographic model can not reproduce the splitting. (c) Model PDF spectrum is recalculated using local structural model in which Pb ion was displaced to (-0.035, -0.023, -0.025). With this model, the doublet is nicely reproduced.

FIG. 4. (a) Temperature dependence of the PDF intensity of PFN at temperatures T=300 K, 200 K, 175 K, 150 K, 125 K, 75 K. Fe/Nb-O bond shows little dependence on temperature. In contrast, PDF peak around r=4 Å exhibits noticeable temperature evolution. (b) Width of the PDF peak at $r \simeq 4.0$ Å. The inset shows the Gaussian fitting at 175 K and 150 K, respectively. To take into account contributions from neighboring peaks, the peak at r = 4 Å and neighboring peaks are simultaneously fitted. The solid line represents a temperature dependence of a square root of mean-square thermal displacement ($\sqrt{2\langle u^2 \rangle}$) calculated using Eq. (2) with Debye temperature Θ_D=145 K.

FIG. 5. Medium-range PDF intensity from T=300 K to 75 K. Note sharp increase of peak height at certain distances and little temperature dependence at other distances.

Figure 1   BX11391   27Dec2010

Figure 2   BX11391   27Dec2010
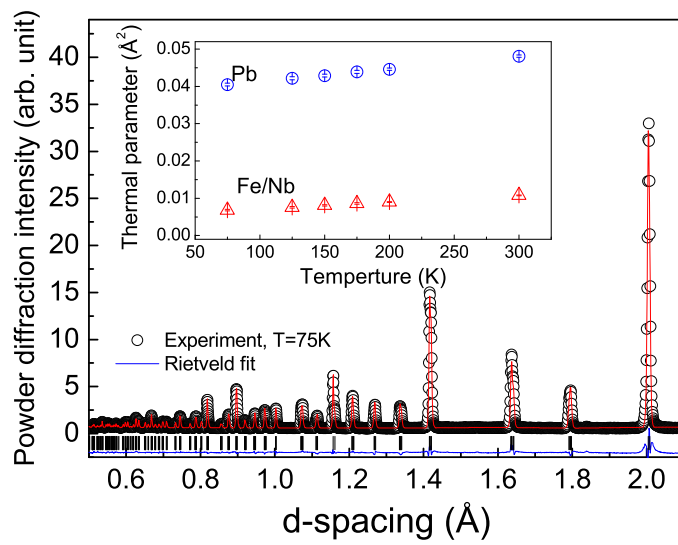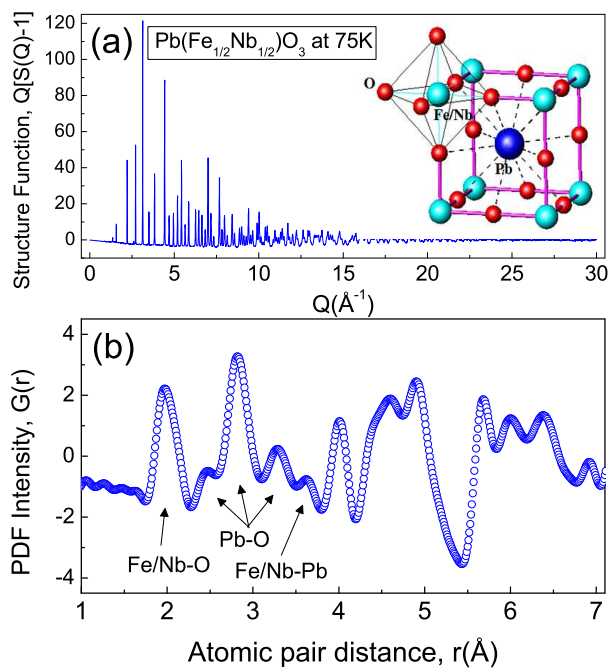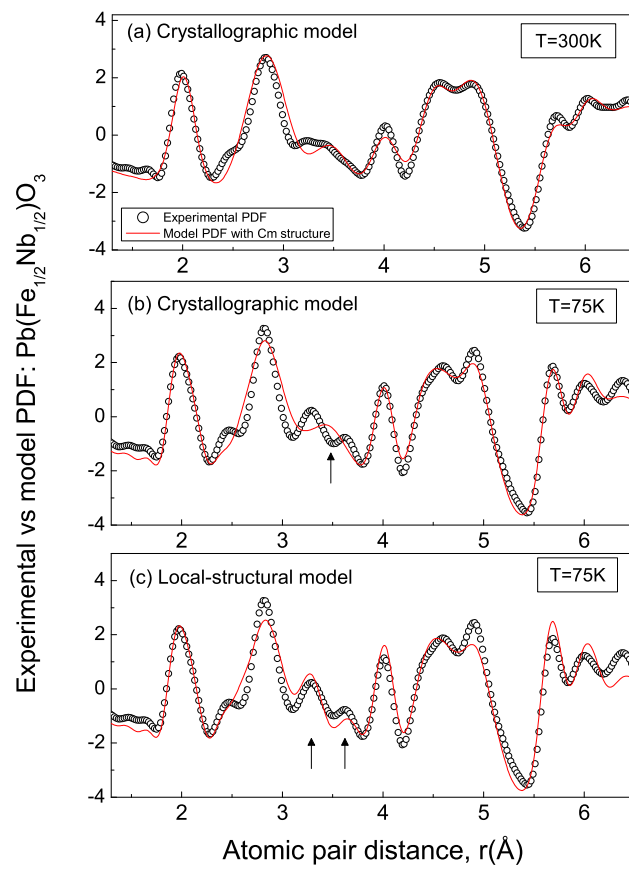
Figure 3   BX11391   27Dec2010
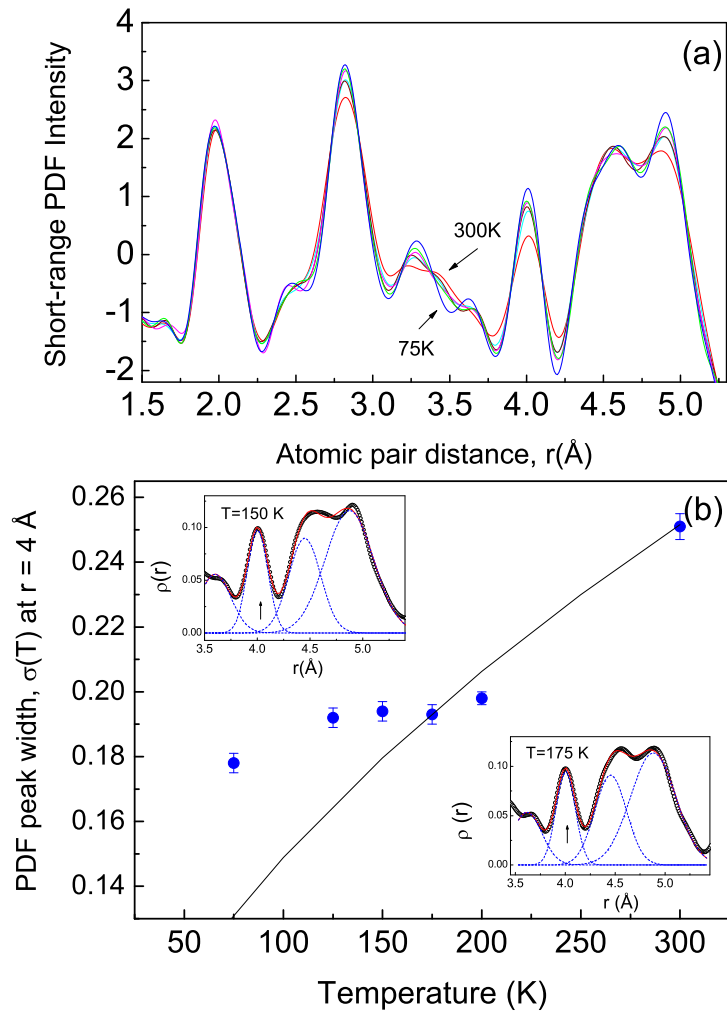
Figure 4   BX11391   27Dec2010
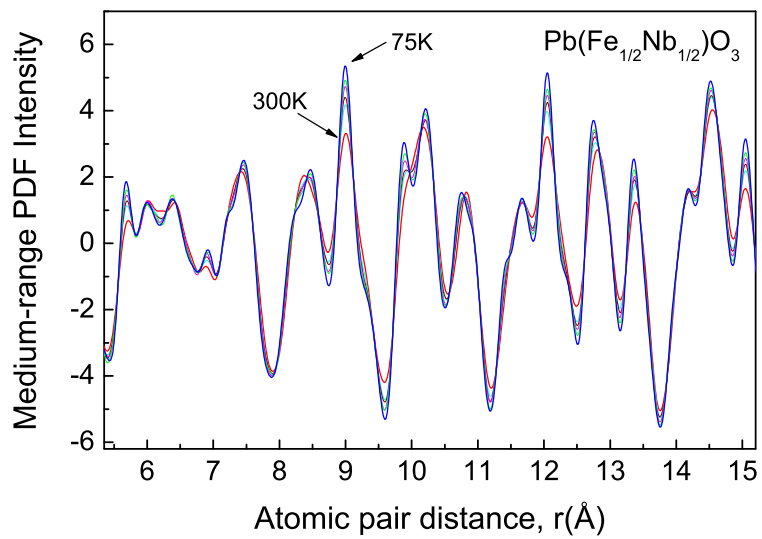
Figure 5   BX11391   27Dec2010